Electrical control of interlayer exciton dynamics in atomically thin heterostructures

Luis A. Jauregui[1], Andrew Y. Joe[1], Kateryna Pistunova[1], Dominik S. Wild[1], Alexander A. High[1,2], You Zhou[1,2], Giovanni Scuri[1], Kristiaan De Greve[1,2], Andrey Sushko[1], Che-Hang Yu[3], Takashi Taniguchi[4], Kenji Watanabe[4], Daniel J. Needleman[3,5,6], Mikhail D. Lukin[1], Hongkun Park[1,2] and Philip Kim[1,3*]

[1] Department of Physics, Harvard University, Cambridge, Massachusetts 02138, USA

[2] Department of Chemistry and Chemical Biology, Harvard University, Cambridge, Massachusetts 02138, USA

[3] John A. Paulson School of Engineering and Applied Sciences, Harvard University, Cambridge, Massachusetts 02138, USA

[4] National Institute for Materials Science, 1-1 Namiki, Tsukuba 305-0044, Japan

[5] Department of Molecular and Cellular Biology, Harvard University, Cambridge, Massachusetts 02138, USA

[6] Faculty of Arts and Sciences Center for Systems Biology, Harvard University, Cambridge, Massachusetts 02138, USA

* To whom correspondence should be addressed: pkim@physics.harvard.edu

Excitons in semiconductors, bound pairs of excited electrons and holes, can form the basis for new classes of quantum optoelectronic devices. A van der Waals heterostructure built from atomically thin semiconducting transition metal dichalcogenides (TMDs) enables the formation of excitons from electrons and holes in distinct layers, producing interlayer excitons with large binding energy and a long lifetime. Employing heterostructures of monolayer TMDs $WSe_2/MoSe_2$, we realize optical and electrical generation of long-lived neutral and charged interlayer excitons. We demonstrate the transport of neutral interlayer excitons across the whole sample that can be controlled by excitation power and gate electrodes. We also realize the drift motion of charged interlayer excitons using Ohmic-contacted devices. The electrical generation and control of excitons provides a new route for realizing quantum manipulation of bosonic composite particles with complete electrical tunability.

Fig. 1

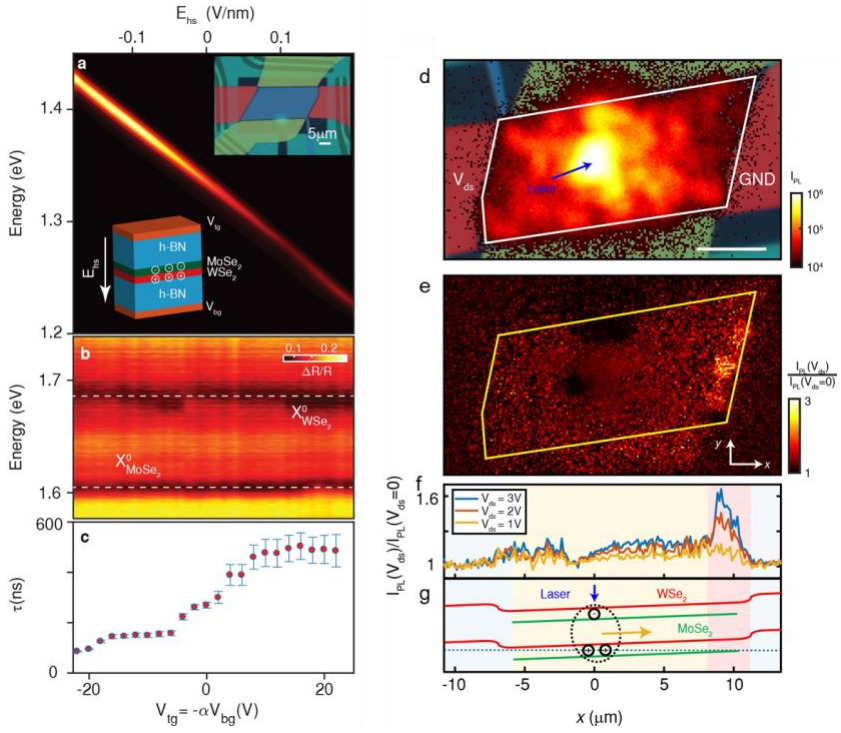

Fig. 1. (a) IE PL spectra vs. electric field applied to the heterostructure ($E_{hs} = (V_{tg} - V_{bg})/t_{total} * (\varepsilon_{h-BN}/\varepsilon_{TMD})$). Here the top ($V_{tg}$) and bottom ($V_{bg}$) gate voltages are swept together with a voltage ratio ($\alpha = t_{top}^{h-BN}/t_{bottom}^{h-BN} = 0.614$, $t_{top}^{h-BN} = 70$ nm and $t_{bottom}^{h-BN} = 114$ nm are the top and bottom *h*-BN thicknesses, respectively), t_{total} is the total *h*-BN thickness, and $\varepsilon_{h-BN} = 3.9$ and $\varepsilon_{TMD} = 7.2$ are the *h*-BN and TMD permittivity, respectively. Right inset: optical image of a representative device with the top-gates false colored. Left inset: schematic of the heterostructure cross section, showing electrons (holes) accumulate on the $MoSe_2$ (WSe_2) layers, forming IEs. The white arrow represents the positive direction of E_{hs}. **(b)** Normalized reflectance vs. E_{hs}. **(c)** IE lifetime τ vs. E_{hs}. **(d)** Spatial dependence of I_{PL} with the laser excitation fixed at the center of the heterostructure (laser position labeled as laser). An optical image of the device with false colored top gates that cover the WSe_2 and $MoSe_2$ contacts is overlaid. An in-plane electric field is applied by a voltage in one of the WSe_2 contacts (V_{ds}) while keeping the other contact grounded. **(e)** Spatial dependence of I_{PL} normalized according to $I_{PL}(V_{ds})/I_{PL}(V_{ds} = 0)$ for V_{ds} = 3 V. We observe a larger population of charged IEs near the right WSe_2 electrode by increasing V_{ds}. The yellow arrow in (d) represents the current direction. **(f)** Average of the normalized I_{PL} along the y-axis vs. *x* (depicted in Figure 3b) for different V_{ds}. **(g)** Schematic of the heterostructure bands with applied V_{ds}. The red (green) bands correspond to WSe_2 ($MoSe_2$). A positive V_{ds} is applied, while the chemical potential (indicated by a blue dotted line) is kept inside the WSe_2 valence band to form positively charged IEs. Under positive V_{ds}, the CIEs drift towards the grounded contact. The emission mainly occurs near the grounded contact, because the charged exciton cannot move beyond the heterostructure.

References

1. L. V. Butov *et al.*, Stimulated scattering of indirect excitons in coupled quantum wells: Signature of a degenerate Bose-gas of excitons. *Phys Rev Lett* **86**, 5608-5611 (2001).
2. M. M. Fogler, L. V. Butov, K. S. Novoselov, High-temperature superfluidity with indirect excitons in van der Waals heterostructures. *Nat Commun* **5**, 4555 (2014).
3. A. A. High *et al.*, Spontaneous coherence in a cold exciton gas. *Nature* **483**, 584-588 (2012).
4. A. A. High *et al.*, Trapping Indirect Excitons in a GaAs Quantum-Well Structure with a Diamond-Shaped Electrostatic Trap. *Phys Rev Lett* **103**, 087403 (2009).
5. L. V. Butov, C. W. Lai, A. L. Ivanov, A. C. Gossard, D. S. Chemla, Towards Bose-Einstein condensation of excitons in potential traps. *Nature* **417**, 47-52 (2002).
6. X. P. Hong *et al.*, Ultrafast charge transfer in atomically thin MoS2/WS2 heterostructures. *Nat Nanotechnol* **9**, 682-686 (2014).
7. P. Rivera *et al.*, Observation of long-lived interlayer excitons in monolayer MoSe2-WSe2 heterostructures. *Nat Commun* **6**, 6242 (2015).
8. D. Unuchek *et al.*, Room-temperature electrical control of exciton flux in a van der Waals heterostructure. *Nature* **560**, 340 (2018).
9. J. S. Ross *et al.*, Electrical control of neutral and charged excitons in a monolayer semiconductor. *Nat Commun* **4**, 1474 (2013).
10. J. S. Ross *et al.*, Interlayer Exciton Optoelectronics in a 2D Heterostructure p-n Junction. *Nano Lett* **17**, 638-643 (2017).
11. C. H. Lee *et al.*, Atomically thin p-n junctions with van der Waals heterointerfaces. *Nat Nanotechnol* **9**, 676-681 (2014).